Journal of Alloys and Compounds 509 (2011) 5853–5857

Contents lists available at ScienceDirect

Journal of Alloys and Compounds

journal homepage: www.elsevier.com/locate/jallcom

Effect of ZrO_2 addition on the microstructure and electromagnetic properties of YIG

Jiaqian Wang[a], Yulong Jin[b], Jian Yang[a], Yinyin Huang[a], Tai Qiu[a,*]

[a] College of Materials Science and Engineering, Nanjing University of Technology, Nanjing 210009, China
[b] Nanjing Institute of Electronic Technology, Nanjing 210039, China

ARTICLE INFO

Article history:
Received 21 July 2010
Received in revised form 23 February 2011
Accepted 27 February 2011
Available online 5 March 2011

Keywords:
Magnetically ordered materials
Solid state reactions
Microstructure
Electromagnetic properties

ABSTRACT

In this work, we reported the microstructure and electromagnetic properties of a series of zirconium substituted yttrium iron garnet ferrites (YCaZrIG) with iron deficiency composition of $Y_{3-x}Ca_xZr_xFe_{4.93-x}O_{12}$ ($x = 0.1$, 0.2, 0.3, and 0.4, with electrostatic balance by Ca^{2+} substituted for Y^{3+} ions) prepared by a solid-reaction method. The addition of ZrO_2 shows no obvious influence on the phase, density and dielectric constant of YIG ferrites. When Zr addition $x \leq 0.3$, the substitution of Zr^{4+} for Fe^{3+} decreases the amount of Fe ions, increases the lattice parameter and enhances the grain growth of garnet phase. The solubility of zirconium in YCaZrIG ferrite was found to be approximately 0.3, above which excess ZrO_2 would lead to the precipitation of a second phase inside the YCaZrIG ferrite. This would inhibit the grain growth of garnet phase and cause an increase in the dielectric loss and coercivity. The observed reduce for saturation magnetization when $x = 0.4$ is possibly due to antiparallel alignment of magnetic moment of Fe^{3+} in the d site caused by the decrease of a–d exchange interaction. Additionally, we got the optimum electromagnetic properties in the samples with $x = 0.3$: $\varepsilon_r = 14.1$, $\tan\delta_e = 2.5 \times 10^{-4}$, $H_c = 47$ A/m, $4\pi M_s = 1936 \times 10^{-4}T$, $\Delta H = 7.1$ KA/m.

1. Introduction

Yttrium iron garnet ($Y_3Fe_5O_{12}$) also known as YIG since its discovery has attracted extensive attention due to its narrow ferromagnetic resonance linewidth, low dielectric loss in microwave regions and important applications in microwave communication devices such as circulators, isolators, gyrators and phase shifters [1]. This compound has three sublattices generally labeled as a [octahedral], d (tetrahedral) and c {dodecahedral}. The c sublattice contains the nonmagnetic rare-earth ions Y^{3+} ($24Y^{3+}$), 16 Fe^{3+} and 24 Fe^{3+} cations fully occupied [a] sites and (d) sites, respectively, which resulted in the high resistivity and small anisotropy constant, consequently the low loss and narrow linewidth. The cation distribution at the [a] and (d) sites of garnet is expected to play the most important role in controlling its magnetic properties. Because of the nonmagnetic ions Y^{3+}, the magnetic contribution of this garnet arises from the antiparallel alignment of the magnetic moments in the [a] and (d) sites. The strongest magnetic interactions in pure YIG is related to the inter-sublattice exchange, i.e., superexchange interaction between Fe^{3+} iron in octahedral and tetrahedral through intervening O^{2-} ions for which the bond angle is 126.6° and the distances $Fe_{[a]}$–O^2, $Fe_{(d)}$–O^2 are 2.00 Å and 1.88 Å, respectively [2]. The interactions between and within sub-lattices of YIG can be tailored by substituting various elements in its structure leading to properties modifications. In this respect, the effect of various substitutions on the microstructure and electromagnetic properties of YIG have been studied [2–19]. Recently, Niyaifar et al. [2] and Xu et al. [3] investigated the effects of indium addition on the structure and magnetic properties of YIG and YBiCaVIG, respectively. They found that appropriate addition of indium can increase saturation magnetization ($4\pi M_s$) and reduce coercivity (H_c) due to the substitution of nonmagnetic ions In^{3+} with larger ionic radius for Fe^{3+} ions in [a] sites. This is significant for the miniaturization and weight reduction of the nonreciprocal microwave devices with lower microwave loss, such as circulators and isolators. However, the raw material In_2O_3 is very expensive, which limits the application of these ferrites. Zr^{4+} is also a kind of nonmagnetic ions and has an ionic radius larger than that of Fe^{3+}, showing a similar character with In^{3+}. Therefore, a similar effect on the properties of YIG would be expected when substituting Fe^{3+} by Zr^{4+} instead of In^{3+}. In addition, the cost of ZrO_2 is much lower than that of In_2O_3. In this investigation, a kind of high performance YCaZrIG ferrite was successfully prepared, in which zirconium was incorporated into YIG to substitute iron ions in [a] sites and calcium was incorporated to substitute Y ions in [c] sites for electrostatic balance. The effect of ZrO_2 addition on the microstructure and electromagnetic properties of $Y_{3-x}Ca_xZr_xFe_{4.93-x}O_{12}$ prepared by conventional solid-state route were investigated. Meanwhile, various techniques such as: X-ray

* Corresponding author. Tel.: +86 25 83587262; fax: +86 25 83587268.
E-mail addresses: qiutai@njut.edu.cn, boleyn-858@163.com (T. Qiu).

0925-8388/$ – see front matter © 2011 Elsevier B.V. All rights reserved.
doi:10.1016/j.jallcom.2011.02.151

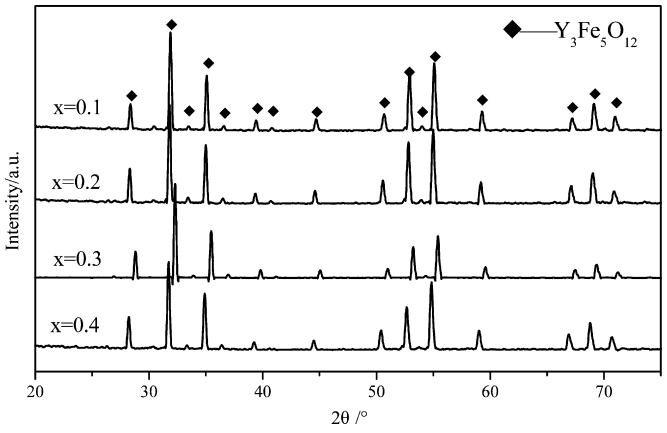

Fig. 1. XRD patterns of YCaZrIG ferrites with different ZrO_2 concentration.

diffraction (XRD), scanning electron microscope (SEM), network analyzer, hysteresigraph, magnetic balance and electron paramagnetic resonance spectrometer were utilized to detect the properties and investigate the mechanism.

2. Experimental

2.1. Sample preparation

The raw materials were Y_2O_3 (99.9% purity), ZrO_2 (99.9% purity), Fe_2O_3 (98% purity) and $CaCO_3$ (99% purity). They were weighed with an accuracy of 0.01 g according to the chosen iron deficiency stoichiometry $Y_{3-x}Ca_xZr_xFe_{4.93-x}O_{12}$ with $x = 0.1$, 0.2, 0.3, and 0.4, and then wet milled in a planetary mill for 6 h with ethanol and ZrO_2 balls. The slurry was then dried and presintered at 1150 °C for 2 h. The presintered mixture was re-milled for 6 h. After being dried, the mixture was pulverized, screened and pressed into cylindrical and ring tablets with specific size. Isostatic pressing technology was also used to improve the density and uniformity of green bodies. Finally, the samples were sintered at 1425 °C for 4 h with a heating rate of 100 °C/h and then naturally cooled to room temperature in air atmosphere.

2.2. Sample characterizations

The bulk density and apparent porosity of the samples was measured using Archimedes' method. The crystalline structure of the sintered samples was determined with XRD technique on ARLX'TRA diffractometer using Cu $K\alpha_1$ radiation in the 2θ angle range between 20 and 75°. The microstructures of the sintered samples were observed by JEOL JSM-5900 scanning electron microscope (SEM) equipped with energy dispersive spectroscope (EDS). The relative dielectric constant ε_r and loss tan δ_e were detected by the modified Hakki and Cole-man's method [20,21] in the TE011 mode using a HP 8722ET network analyzer at a frequency between 8 GHz and 12 GHz. The magnetic properties (H_c and $4\pi M_s$) were measured using KJS ASSOCIATES SMT-600 hysteresigraph and magnetic balance. Hysteresis loop was measured at 300 Hz. The ferromagnetic resonance linewidth ΔH was measured using the Bruker EMX-10/12 Electron Paramagnetic Resonance Spectrometer at 9.7767 GHz.

3. Results and discussion

3.1. Phase analysis and sintering character

Fig. 1 shows the XRD patterns of the samples with different ZrO_2 addition. As can be identified from these patterns, the formation of garnet phase was confirmed for all the samples synthesized. Increase in the magnitude of x leads to variation in the lattice parameters of the samples (seen in Fig. 2), which were calculated by a Cohen canonical equation shown as follows [22]:

$$\sum a \sin^2\theta = A\sum a^2 + C\sum a\delta$$

$$\sum \delta \sin^2\theta = A\sum a\delta + C\sum \delta^2 \quad (1)$$

where $A = \lambda^2/4a_0^2$, $a = (h^2 + k^2 + l^2)$, $C = D/10$, $\delta = 10\sin^2 2\theta$, D is the particle size.

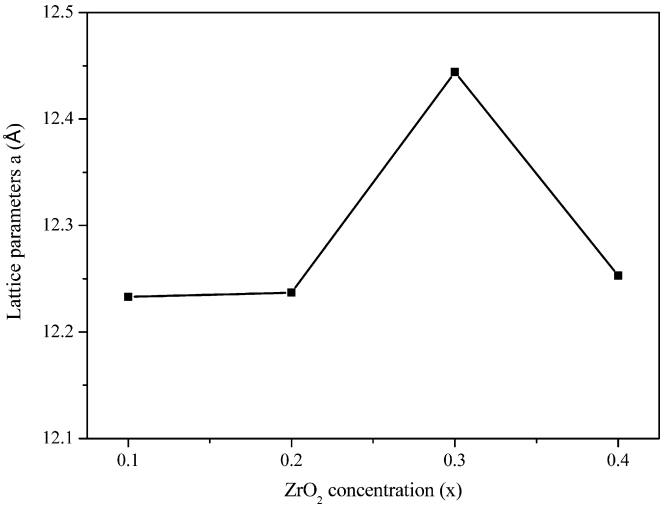

Fig. 2. Lattice parameters of YCaZrIG ferrites with different ZrO_2 concentration.

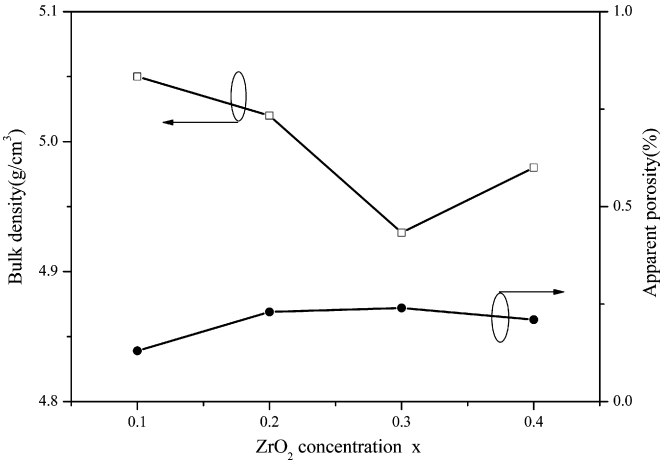

Fig. 3. Sintering performance of YCaZrIG ferrites with different ZrO_2 concentration.

The values of lattice parameter increase with the increase of ZrO_2 addition firstly, which can be explained by considering the larger ionic radius of Zr^{4+} (0.80 Å) compared with that of Fe^{3+} (0.64 Å). However, a decrease in lattice parameters was found when the ZrO_2 addition x is 0.4.

Fig. 3 gives the bulk density and apparent porosity of the samples with different ZrO_2 addition. As illustrated in this figure, all the samples show a high sintering density (apparent porosity is lower than 0.25%), suggesting that all the samples were densified and the ZrO_2 addition has little influence on the densification of the samples. However, the bulk density decreases with ZrO_2 addition when $x \leq 0.3$. As has been mentioned above, the lattice parameters of the samples increase with x increasing. According to the equation $\rho = ZW_m/N_A a^3$ (ρ is the theoretical density, Z is the number of molecules per unit cell of the garnet structure, W_m is the molecular weight, and N_A is Avogadro's constant) [10], the decrease in bulk density can be easily attributed to the decrease in theoretical density caused by the substitution of Zr^{4+} for Fe^{3+}. However, the bulk density shows a minor increase when x is above 0.3, which may be related to the formation of a second phase with a higher density [shown in Fig. 4(d)].

3.2. Microstructure analysis

Fig. 4 shows the SEM micrographs of the polished surface of the samples after hot corrosion. As can be seen in Fig. 4, few pores can

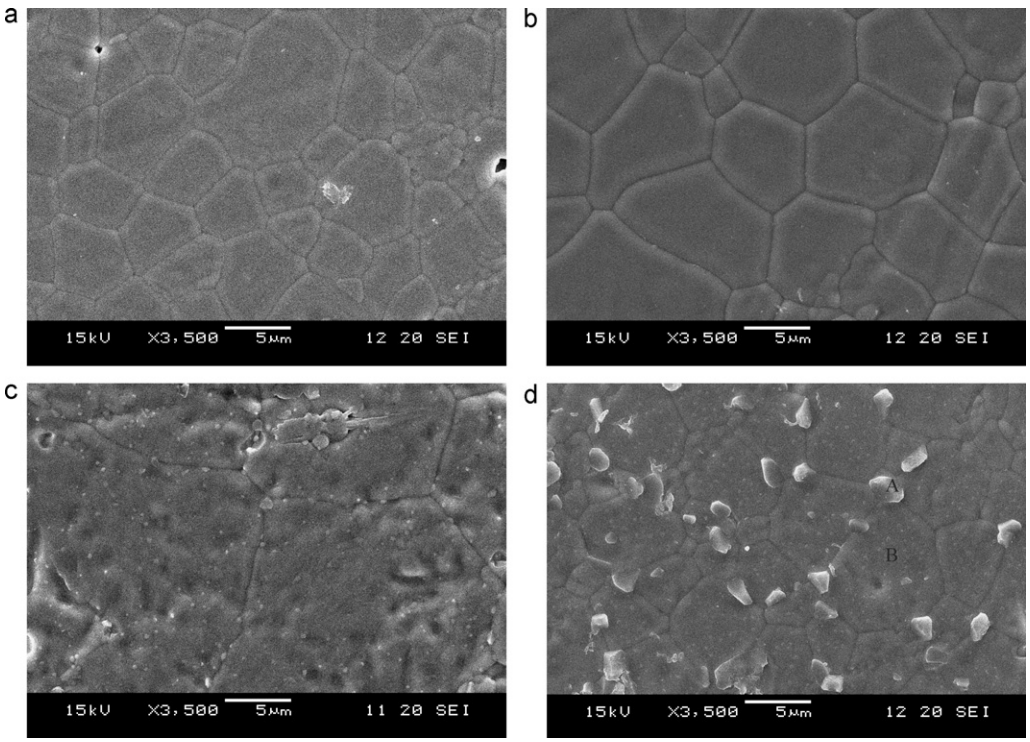

Fig. 4. SEM micrographs of YCaZrIG ferrites with different ZrO_2 concentration (a) $x = 0.1$; (b) $x = 0.2$; (c) $x = 0.3$; (d) $x = 0.4$.

be observed, which also confirmed the high density of all the samples. The average grain size of the samples increases gradually with the increasing Zr content. The YCaZrIG ferrite with $x = 0.3$ shows the maximum grain size of about 15 μm. When Zr content was increased to 0.4, the average grain size decreases and some smaller grains appear at the grainboundaries of YCaZrIG ferrite. Fig. 5 displays the EDS analysis of YCaZrIG ferrite with x = 0.4. EDS analysis on many grains in Fig. 4(d) (sample with $x = 0.4$) reveals that the smaller grains (represented by A) obviously have a different composition compared with the main crystal phase (represented by B). Thus, it can be suggested that a second phase will precipitate when excess Zr is incorporated, which can prevent the mobilization of the grainboundary and inhibit the grain growth of garnet phase. By combing the variation of lattice parameters, it is possible that the solid solubility limit of Zr^{4+} in this ferrite is 0.3, above which the surplus Zr^{4+} cannot enter the crystal lattice of garnet and will distribute in the grain boundary to form a second phase. As the amount of the second phase is small, it was not detected in XRD analysis.

3.3. Dielectric properties

Fig. 6 demonstrates the dielectric properties of YCaZrIG ferrites prepared in this work. As can be seen from this figure, the addition of ZrO_2 shows no influence on the dielectric constant of the samples, which varies between 14.1 and 14.7. The magnitude of $\tan\delta_e$ exhibits a sharp drop firstly and then a weak increase with the increase of ZrO_2 addition. The samples with $x = 0.2$ and 0.3 shows the lowest dielectric loss of 2.5×10^{-4}. Liao et al. [23] has found that the directional polarization relaxation of intrinsic electric dipole and interfacial polarization relaxation are the main resources of microwave dielectric loss in polycrystalline ferrites. They pointed out that the chief way of lowering the microwave dielectric loss of polycrystalline ferrites are (1) to restrain the production of vacancies in the crystal and the entering of impurity ions of higher and lower valency into the crystal, and to avoid the occurring of high conductive phases; (2) to reduce the macroscopic and microscopic heterogeneities (e.g., pores, inclusions and grainboundary, etc.); (3) to promote grain growth and reduce the amount of grainboundary. The phenomenon in this work can be attributed to the substitution of Zr^{4+} for iron cations at octahedral [$16Fe^{3+}$]

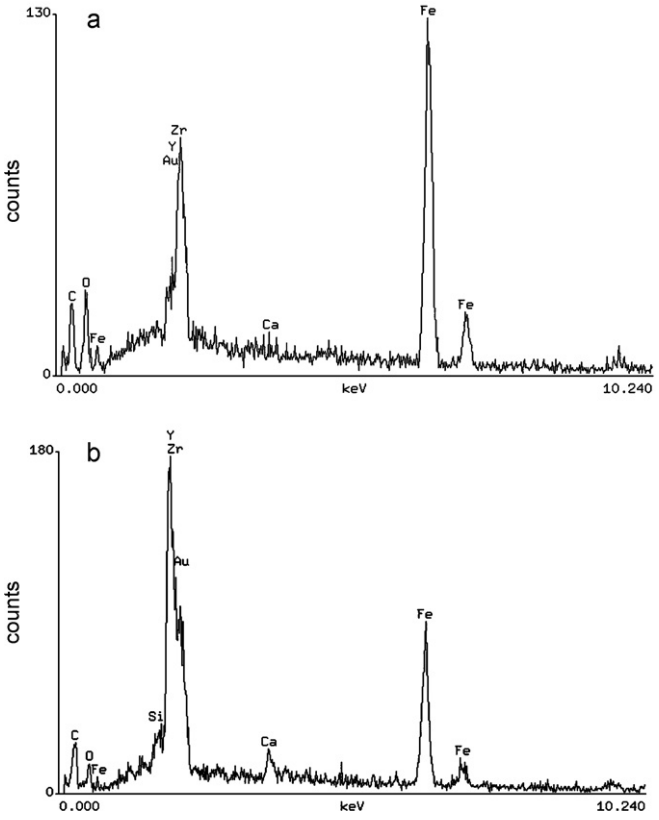

Fig. 5. EDS analysis of YCaZrIG ferrite with $x = 0.4$: (a) EDS of A (small grains) in Fig. 4(d); (b) EDS of B (large grains) in Fig. 4(d).

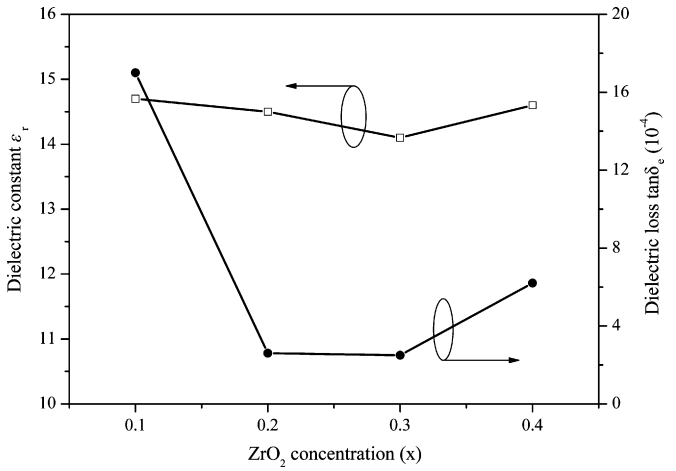

Fig. 6. Dielectric properties of YCaZrIG ferrites with different ZrO_2 concentration.

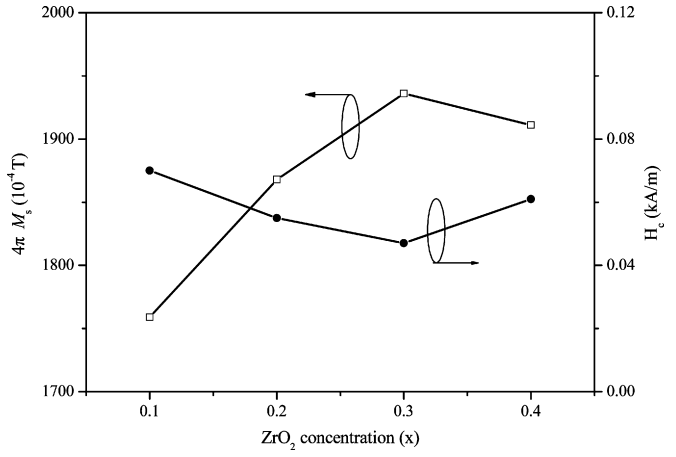

Fig. 7. Magnetic properties of YCaZrIG ferrites with different ZrO_2 concentration.

sites. Although the substitution of Zr^{4+} increases the lattice parameters and brings more deficiencies, it reduces the total amount of iron cations (including Fe^{3+} and Fe^{2+}). Meanwhile, the partial substitution of Zr^{4+} for Fe^{3+} ions enhances the grain growth and reduces the amount of grain boundary (seen in Fig. 4). As a result, the dielectric loss decreases. However, when the doping amount of ZrO_2 exceeds a critical amount (the solid solution limit), a second phase precipates at the grainboundary and hinders the mobilization of grainboundaries during densification process, which results in the increase in dielectric loss.

3.4. Magnetic properties

Fig. 7 displays the variations of the room temperature saturation magnetization ($4\pi M_S$) and coercivity (H_c) with ZrO_2 concentration (x) for the YCaZrIG ferrites prepared in this work. As can be seen from this figure, the coercivity decreases with the increasing ZrO_2 concentration and reaches the minimum of 47 A/m at $x = 0.3$. However, when x is above 0.3, the coercivity shows a weak increase. This phenomenon also can be related to the substitution of Zr^{4+} for iron cations at octahedral [$16Fe^{3+}$] sites, which induced crystal grain growth. The coercivity is decided by the facility of magnetic domain wall motion and magnetic moment reverse [24]. As can be seen from Fig. 4, with x increased from 0.1 to 0.3, the crystal grain size increases notably. As a result, the abilities of magnetic domain wall migration and the magnetic moment reverse are enhanced and so coercivity decreases. The latter rise of coercivity when $x > 0.3$ can be attributed to the formation of a second phase in the grain boundary (seen in Fig. 4), which increases magnetocrystalline anisotropy constant K_1 to raise domain wall energies and impede wall motion [16]. As to saturation magnetization, it increases with ZrO_2 addition increasing and reaches the maximum of $1936 \times 10^{-4}T$ at $x = 0.3$, which is followed by a decrease when x is 0.4. Based on Neel's theory of ferrimagnetism in ferrites [25], the substitution of a non-magnetic ion like Zr^{4+} in [a] site can lead to the rise of total saturation magnetization. However, the observed decline in saturation magnetization for the sample with $x = 0.4$ may be attributed to the formation of a special d site when the addition of Zr^{4+} surpasses a critical limit ($x = 0.3$), in which all the magnetic positive ions will lose the object of superexchange interaction because of the position occupied by Zr^{4+}. This will lead to the decrease of a–d exchange interaction. Meanwhile, d–c, d–d exchange interaction will increase, which will result in magnetic moment of Fe^{3+} anti-parallel alignment in the d site [3]. As a result, saturation magnetization shows a little decrease.

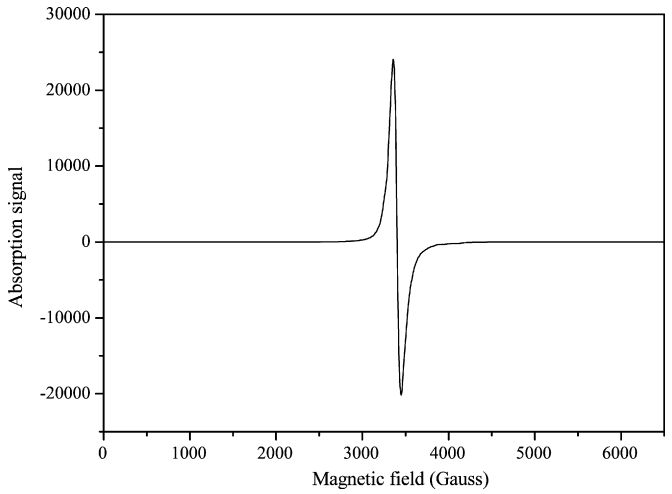

Fig. 8. Ferromagnetic resonance curve of the $Y_{2.7}Ca_{0.3}Zr_{0.3}Fe_{4.63}O_{12}$ ferrite at 9.7767 GHz.

As the YCaZrIG ferrite with $x = 0.3$, i.e., $Y_{2.7}Ca_{0.3}Zr_{0.3}Fe_{4.63}O_{12}$ shows the optimum electromagnetic properties, ΔH, the important parameter of microwave magnetic material concerns the magnetic losses, of the material was also measured. Fig. 8 shows the ferromagnetic resonance curve of the $Y_{2.7}Ca_{0.3}Zr_{0.3}Fe_{4.63}O_{12}$ ferrite at 9.7767 GHz, from which ΔH was determined to be 7.1 KA/m (89.2 Gs).

3.5. Application in microwave devices

The YCaZrIG ferrites with the optimum electromagnetic properties (i.e., $Y_{2.7}Ca_{0.3}Zr_{0.3}Fe_{4.63}O_{12}$) in this work was send to Nanjing Institute of Electronic Technology to measure the operational performance in microwave devices (isolators). A low insert loss ($\leq$0.35 dB) and higher isolation ($\geq$22 dB) were obtained, which can satisfy the requirements perfectly and suggests a promising application prospect.

4. Conclusions

The addition of ZrO_2 shows no obvious influences on the phase, density and dielectric constant of YIG ferrites. When ZrO_2 addition $x \leq 0.3$, the substitution of Zr^{4+} for Fe^{3+} decreases the amount of Fe ions, increases the lattice parameter and enhances the grain growth of garnet phase. The solubility of zirconium in YCaZrIG ferrite was found to be approximately 0.3, above which excess ZrO_2 would lead to the precipitation of a second phase inside the YCaZrIG fer-

rite. This would inhibit the grain growth of garnet phase and cause an increase in the dielectric loss and coercivity. Nevertheless, the observed reduce for saturation magnetization when $x = 0.4$ is possibly due to antiparallel alignment of magnetic moment of Fe^{3+} in the d site caused by decrease of a–d exchange interaction. Therefore, proper quantities of ZrO_2 addition into YIG ferrite could not only improve the electromagnetic properties ($\tan\delta_e$ and H_c), but also hold a higher saturation magnetization. The YCaZrIG ferrite with $x = 0.3$, i.e., $Y_{2.7}Ca_{0.3}Zr_{0.3}Fe_{4.63}O_{12}$ shows the optimum electromagnetic properties: $\varepsilon_r = 14.1$, $\tan\delta_e = 2.5 \times 10^{-4}$, $H_c = 47$ A/m, $4\pi M_s = 1936 \times 10^{-4}T$, $\Delta H = 7.1$ KA/m.

References

[1] V.G. Harris, A. Geiler, Y.J. Chen, S.D. Yoon, M.Z. Wu, A. Yang, Z.H. Chen, P. He, P.V. Parimi, X. Zuo, C.E. Patton, M. Abe, O. Acher, C. Vittoria, J. Magn. Magn. Mater. 321 (2009) 2035–2047.
[2] M. Niyaifar, A. Beitollahi, N. Shiri, M. Mozaffari, J. Amighian, J. Magn. Magn. Mater. 322 (2010) 777–779.
[3] Q.M. Xu, W.B. Liu, L.J. Hao, C.J. Gao, X.G. Lu, Y.A. Wang, J.S. Zhou, J. Magn. Magn. Mater. 322 (2010) 2276–2280.
[4] Y.J. Wu, R.Y. Hong, L.S. Wang, G.Q. Di, H.Z. Li, B. Xu, Y. Zheng, D.G. Wei, J. Alloys Compd. 481 (2009) 96–99.
[5] C.S. Kim, B.K. Min, S.J. Kim, S.R. Yoon, Y.R. Uhm, J. Magn. Magn. Mater. 254–255 (2003) 553–555.
[6] S. Geller, R.C. Sherwood, G.P. Espinosa, H.J. Williams, J. Appl. Phys. 36 (1) (1964) 321.
[7] X. Zhang, H.Z. Lin, IEEE Trans. Magn. 19 (3) (1983) 1457–1463.
[8] M. Gasgnier, J. Ostoréro, A. Petit, J. Alloys Compd. 275–277 (1998) 41–45.
[9] Z.J. Cheng, H. Yang, Physica E 39 (2007) 198–202.
[10] T.C. Mao, J.C. Chen, J. Magn. Magn. Mater. 302 (2006) 74–81.
[11] S. Geller, H.J. Williams, R.C. Sherwood, G.P. Espinosa, J. Phys. Chem. Solids 23 (11) (1962) 1525–1540.
[12] Z.J. Cheng, H. Yang, Y.M. Cui, L.X. Yu, X.P. Zhao, S.H. Feng, J. Magn. Magn. Mater. 308 (2007) 5–9.
[13] G.F. Dionne, J.B. Goodenough, Mater. Res. Bull. 7 (1972) 749–760.
[14] C.E. Patton, Phys. Rev. 179 (2) (1969) 352–358.
[15] M. Sugimoto, J. Am. Ceram. Soc. 82 (2) (1999) 269–280.
[16] G.F. Dionne, Proc. IEEE 63 (5) (1975) 777–789.
[17] I.I. Davidenko, J. Alloys Compd. 369 (2004) 166–169.
[18] A. Kianvash, R. Arghavanian, S. Zakerifar, M. Sheykholeslami, J. Alloys Compd. 461 (2008) 432–435.
[19] S.D.S. Marins, T. Ogasawara, A.S. Ogasawara, J. Alloys Compd. 436 (2007) 415–420.
[20] B.W. Hakki, P.D. Coleman, IEEE Trans. Microwave Theory Technol. 8 (4) (1960) 402–410.
[21] Y. Kobayshi, M. Katoh, IEEE Trans. Microwave Theory Technol. 33 (7) (1985) 586–592.
[22] N.L. Yang, Test Method of Inorganic Materials, first ed., Wuhan University of Technology Press, Wuhan, 1990.
[23] S.B. Liao, G.J. Yin, J. Liu, Acta Scientiarum Naturalium Universitatis Pekinensis (China) 3 (1979) 52–65.
[24] A. Globus, P. Duplex, M. Guyot, IEEE Trans. Magn. 7 (3) (1971) 617–621.
[25] J.S. Smart, Am. J. Phys. 23 (6) (1955) 356–370.